



**SINERGI** Vol. 25, No. 2, June 2021: 159-168  
<http://publikasi.mercubuana.ac.id/index.php/sinerigi>  
<http://doi.org/10.22441/sinerigi.2021.2.007>



## EXPERIMENTAL MODEL OF SINGLE-PHASE DC-DC BOOST CONVERTER FOR 1000 WP PHOTOVOLTAIC APPLICATION

Handoko Rusiana Iskandar<sup>1\*</sup>, Muhammad Rizky Alfarizi<sup>1</sup>, Ajie Prasetya<sup>1</sup>, Nana Heryana<sup>2</sup>

<sup>1</sup>Department of Electrical Engineering, Faculty of Engineering, Universitas Jenderal Achmad Yani, Indonesia

<sup>2</sup>Electrical Energy Conversion Research Laboratory, School of Electrical Engineering and Informatics, Bandung Institute of Technology, Indonesia

### Abstract

The photovoltaic system is used and utilized as electricity demand in many developed countries, including Indonesia. Nowadays, the photovoltaic system is an alternative source of inexpensive, reasonably priced electricity and easily applied in public facilities until laboratory usage. In Electrical Engineering Laboratory (EEL), Faculty of Engineering (FoE), Universitas Jenderal Achmad Yani is 1 kWp peak photovoltaic application available. The PV system is planned to be connected to the grid and produces 220VAC / 50Hz characteristics to meet the existing load capacity. The PV systems modeled include Pulse Width Modulation (PWM) controlled DC/DC Boost Converter, and DC/AC converter circuit. This study's experimental architecture is proposed to meet the electrical load following the characteristics of the photovoltaic device. The three types of electronic switching control, namely Metal Oxide Semiconductor Field Effect Transistor (MOSFET), Insulated Gate Bipolar Transistor (IGBT) and Gate Turn-off Thyristor (GTO), are used to achieve the highest performance. Based on the 1 kWp photovoltaic system's simulation results from the three types of electronic power switching, a minimum output voltage range of 210-230 VDC is produced. DC/AC Converter testing has been carried out and can be tested on a grid-connected 220VAC/50Hz single phase with the highest output using MOSFET equal to 96.7%.

This is an open access article under the [CC BY-NC](https://creativecommons.org/licenses/by-nc/4.0/) license



### Keywords:

Boost Converter;  
MOSFET;  
Pulse Wave Modulation;  
Photovoltaic System;  
Single-phase;

### Article History:

Received: June 21, 2020

Revised: July 28, 2020

Accepted: August 4, 2020

Published: February 10, 2021

### Corresponding Author:

Handoko Rusiana Iskandar  
Department of Electrical Engineering, Faculty of Engineering, Universitas Jenderal Achmad Yani  
Email: [handoko.rusiana@lecture.unjani.ac.id](mailto:handoko.rusiana@lecture.unjani.ac.id)

### INTRODUCTION

Inevitably, fossil fuels are immediately replaced by renewable energy. The Photovoltaic (PV) system is one of them. A PV converts solar energy into electricity and is environmentally friendly energy. The essential element of a PV system is a PV cell that can be grouped as arrays. The voltage and current available on PV directly power the load connected to the grid using an appropriate energy conversion device [1]. Public facilities use this advantage to the research laboratory [2][3].

This paper certainly cannot be separated from several existing studies, including about calculating energy losses in PV panels, calculation techniques and voltage drop to output power suitability by [4][5]. Electrical Engineering

Laboratory (EEL), Faculty of Engineering (FoE), Universitas Jenderal Achmad Yani (UNJANI) available stand-alone PV system. Based on studies, PV systems must always operate at the MPP to get the energy benefits in the optimum state without shading. If shading is taken into account, this PV system has losses due to the shading effect of around 20.8%. The maximum peak power will drop to 792 Wp [6]. The energy produced by PV panels is highly volatile. It is greatly influenced by climatological conditions around the PV, such as solar irradiation and ambient temperature so that the characteristics of the current and voltage generated by PV vary [7][8]. Because of PV panels' unique characteristics, PV panels are not directly connected to the load but use a DC/DC converter

circuit to connect the PV panels and the existing load. PV panels have a maximum power point (MPP) when the current and voltage are at their maximum value.

MPPT is a method used to maximize solar energy acquisition to the output performance of voltage, current and power that is typical of PV [9][10]. MPPT also acts as an electronic system operated by a PV panel so that the PV system can produce maximum power. The PV system then needs a grid connected inverter component so that the PV module can send power to the grid. The thing to do is to interconnect the direct current voltage to the alternating current voltage, one of which is the electronic power converter functions to convert it. Analysis and losses on the PV power rating are mapped by the influence of irradiance and varying temperatures and the efficiency of the converter when in the existing condition of a grid-connected PV application system [11].

The power generated from grid-connected PV systems is used to meet the local loads. If the local load is greater than the PV power, the network meets the remaining power requirements. Conversely, if the local load is less than the power generated by PV, then the PV power is sent to the grid. Systems that are connected to the grid must have good quality AC and the same as those provided by PLN. To ensure that the electricity, it is necessary to design an inverter suitable for the characteristics of the grid-connected PV application [12][13].

This paper will discuss a DC/DC Converter scheme and compare the performance of three types of power electronic switches to meet the 220VAC / 50Hz grid-connected PV criteria of a 1 kWp PV system EEL. The power electronic switches used are Metal Oxide Semiconductor Field Effect Transistors (MOSFETs), Insulated Gate Bipolar Transistors (IGBT), and Gate Turn-off Thyristors (GTO) on DC/AC converter. According to the standard, these three components are tested experimentally using models and simulations with supporting component values that approach the simulation results.

## METHOD

### Design of PV Panel and Specification

The peak power is obtained by multiply the current with the voltage of PV panels. Table 1 shows the (Vmp) max. The voltage from one panel to load the 18 VDC voltage is configured in series, so from the 10 PV panels is 180 VDC multiplied by the nominal current on the PV [14][15]. Follow by (1) – (3),

$$V_{mp_{total\_series}} = \sum_n^i = 1 V_{mp_n} \quad (1)$$

$$I_{mp_{total\_series}} = 1 V_{mp_n} \quad (2)$$

$$P_{mp} = V_{mp} . I_{mp} \quad (3)$$

Table 1. Technical Data of PV Parameters

| No | Nameplate              | Details             |
|----|------------------------|---------------------|
| 1  | PV Cell Technology     | Si-mono Crystalline |
| 2  | Max. Operation Voltage | $V_{mp}$ 18 V       |
| 3  | Max. Operation Current | $I_{mp}$ 5.56 A     |
| 4  | Short Circuit Current  | $I_{sc}$ 6.02 A     |
| 5  | Open Circuit Voltage   | $V_{oc}$ 22.36 V    |

### Modeling of PV Characteristics

The PV system characteristics parameters can be determined by modeling the specifications of the existing PV panels based on Table 1. The Characteristics of PV panels are tested through the current to voltage (I-V) including open-circuit voltage ( $V_{oc}$ ), short circuit current ( $I_{sc}$ ), and PV output power (P-V). The equivalent circuit and the characteristic of the PV cell shown in Figure 1 and (4) [16][17]. Equation (4) shows  $I_{pv}$  and  $V_{pv}$  for the output voltage and current of the PV cell,  $I_{ph}$  is the current resulting from the alluring photon force [18]. Whereas, the diode saturation current is modeled, which shows the characteristics of the diode.  $q$  is the electron charge, and  $n$  is an ideal factor,  $k_B$  is the Boltzmann constant, then the temperature (T) of the solar cell (°K),  $R_p$  is the shunt resistance with a leakage current that passes the path into the cell.  $R_s$  is a shunt resistance that shows a decrease from within a series [19]. All of this relates to the maximum amount of current and voltage that can be produced from solar cells.

$$i_{pv} = i_{ph} - i_o \left[ \exp\left(\frac{v_{pv} + i_{pv}R_s}{nk_B T/q}\right) - 1 \right] - \frac{v_{pv} + i_{pv}R_s}{R_p} \quad (4)$$

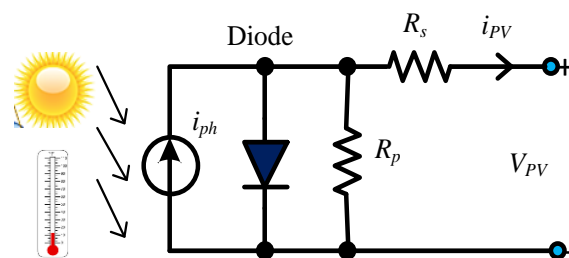


Figure 1. Equivalent Circuit of Single Cell

**Modeling and Simulation Concept  
DC/DC Boost Converter**

DC-DC Boost Converter is an electronic switching circuit that can turn a direct voltage source into a large voltage and adjustable frequency. Voltage regulation outside the converter is performed by adjusting the voltage variation in the input converter's direction. The voltage control of the converter is known as Pulse Width Modulation (PWM) [20]. DC-DC Boost Converter is a static device that is used to produce a variable voltage from a fixed directional voltage source. This circuit is used to transform low directional voltage to high directional voltage which can be converted to a variable voltage [21].

Research related to the background and analysis as well as the relationship with previous research is the simulation of Power Point Tracking on PV panels using Simulink/Matlab R2017a. PWM style controllers use electronic power components in DC/DC conversion circuits for monitoring the PV module MPP or I-V PV curve series. The controller monitors the charging conditions and pulse change. PV panels using MPPT systems produce greater output power than PV panels without MPPT [22][23]. To meet these criteria, the converter circuit is simulated using a DC voltage source (VS), MOSFET as Switch (S), inductor (L), a diode (D), load resistance (RL) and capacitor (C). Where (IO) the output current, (VO) is the output voltage [24][25]. The circuit is tested and compared on each component of power electronics.

**DC/AC Converter (Inverter)**

Figure 2 shows the PV Input in Standard Test Condition (STC) at Irradiance 1000 W/m<sup>2</sup> and temperature 25°C. Design a DC/DC Boost Converter with an output voltage of 220 VDC. Then model the DC/AC converter/inverter to change the DC voltage to AC and the grid connected to PLN 220VAC/50Hz. Grid-connected inverters have specific standards because these inverters are connected to a large power system grid. The standard for grid-connected inverters is written in IEC61727, IEEE1547 and SPLN shows the standard voltage and frequency for grid-connected inverters listed in Table 2 [21].

Table 2. Standard voltage and frequency range

| Normal Rating | IEC61727    | IEEE1547         | SPLN 1:1995 |
|---------------|-------------|------------------|-------------|
| Volt.         | 85% - 110%  | 88% - 110%       | 5% - 10%    |
| Freq.         | 50 +/- 1 Hz | 59,3Hz – 60,5 Hz | 50 Hz       |

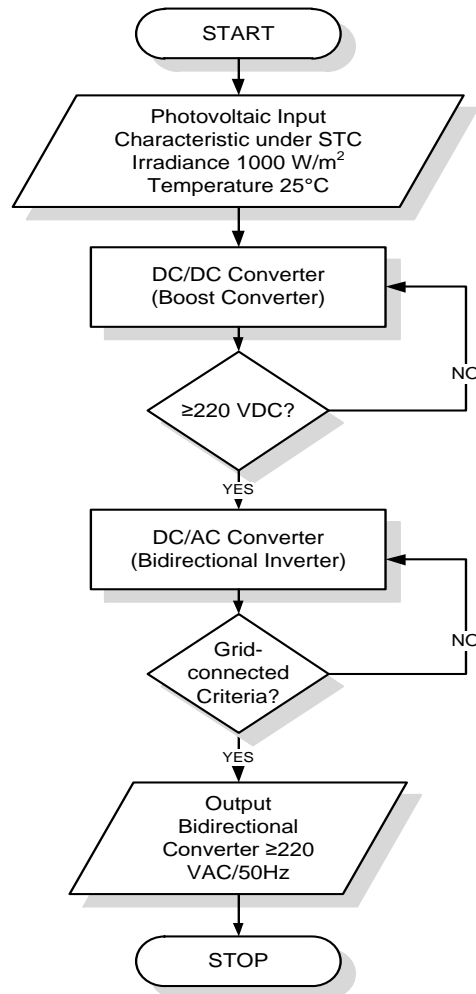


Figure 2. Flowchart Model and Simulation

**RESULTS AND DISCUSSION  
Result of PV Characteristics**

The calculation of the system configuration using (1) – (3) produces a maximum power of 1000.8 Watt peak. In this simulation, the PV panels are connected in series to produce large voltages while the current remains at its nominal value according to Table 1. The installation used on PV panels can be seen in Figure 3.

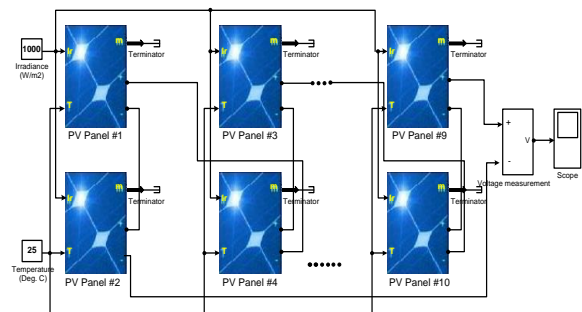


Figure 3. 1 kWp Array Configuration

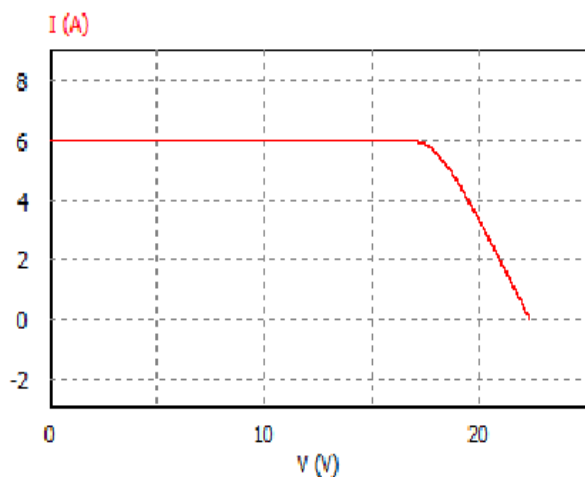


Figure 4. Characteristic curves of I-V

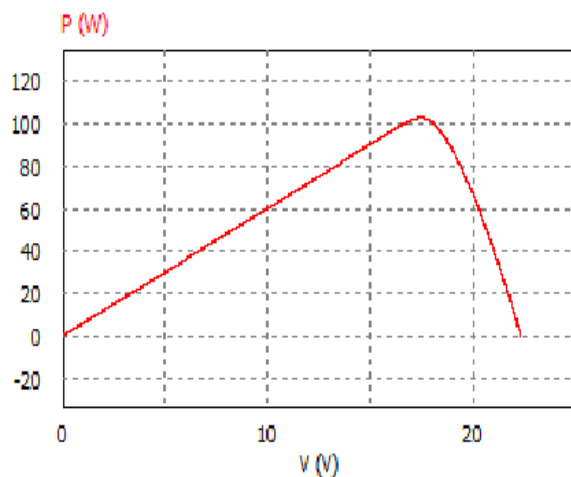


Figure 5. Characteristic curves of P-V

Figure 4 indicates that the current and voltage properties are the product of the efficacy of the linear radiation as the panel current is pushed in its full state (as short-circuited) the voltage falls to zero. Figure 5 reveal that the PV cells have a typical voltage source on the I-V curve's right side, where the output voltage is almost constant. In comparison, the current source action is tested on the left side of the I-V curve. Indicates a utilized spot where the output power will be able to optimize. This operating point is well known with Maximum Power Point (MPP) on STC when  $1000 \text{ W/m}^2$  and Temperature  $25^\circ\text{C}$ .

Figure 6 shows the proposed simulation block, which is done through a library that already exists on Simulink. The PV system scheme is modeled as a whole and each block consists of 4 stages, ranging from PV panel blocks, Boost Converter blocks, PWM control blocks and DC/AC converter inverter blocks. Each has functions and sub-programs. The output waveform is displayed through the block function of the scope and easily displays each block's current and voltage. The controller is designed to generate the amount of output produced. The results of this test are based on varying amounts of solar irradiance.

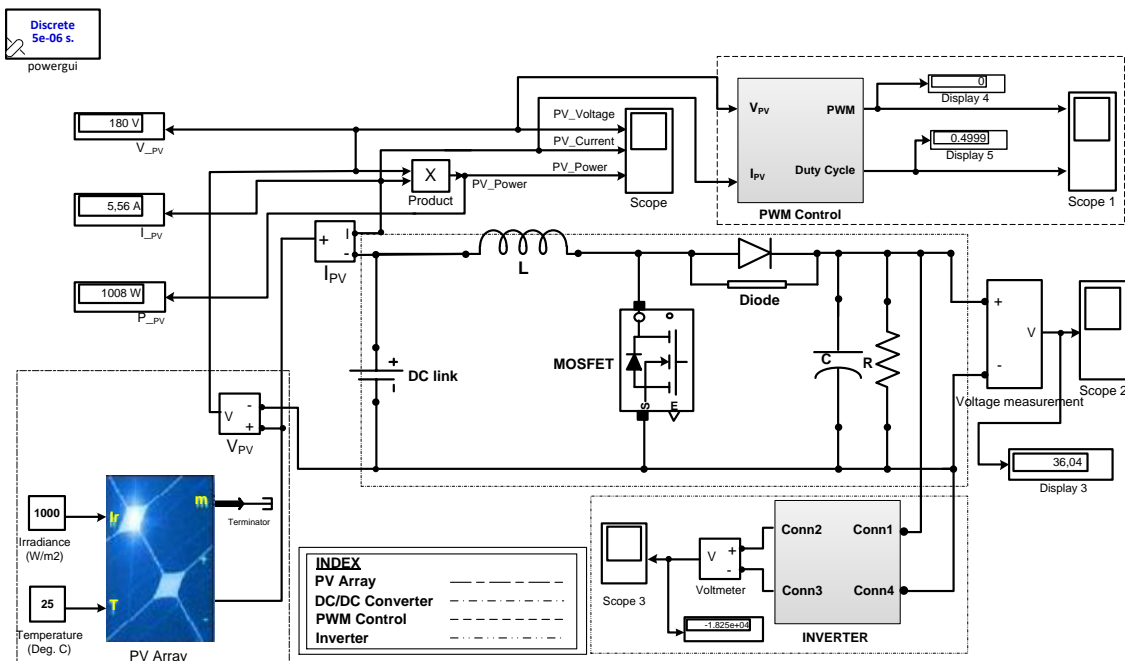


Figure 6. Scheme of Simulation using SIMULINK/MATLAB R2017a

**Modeling of DC/DC Converter**

As shown in the simulation result in Figure 7, the switching process occurs when the switch gate (S) opens, the diode polarization will co-occur. The Inductor voltage (L) then advances to the main source voltage ( $V_s$ ), giving an output voltage ( $V_o$ ) greater than ( $V_s$ ) the main source and

experiencing reinforcement with the same polarity. Thus, the load ( $R_L$ ) is fed by the inductor (L) and the source voltage ( $V_s$ ). PWM and MPPT controllers generally use the series-type or shunt controller feature. After the Boost Converter process is then forwarded to the inverter block, it then converts to AC voltage.

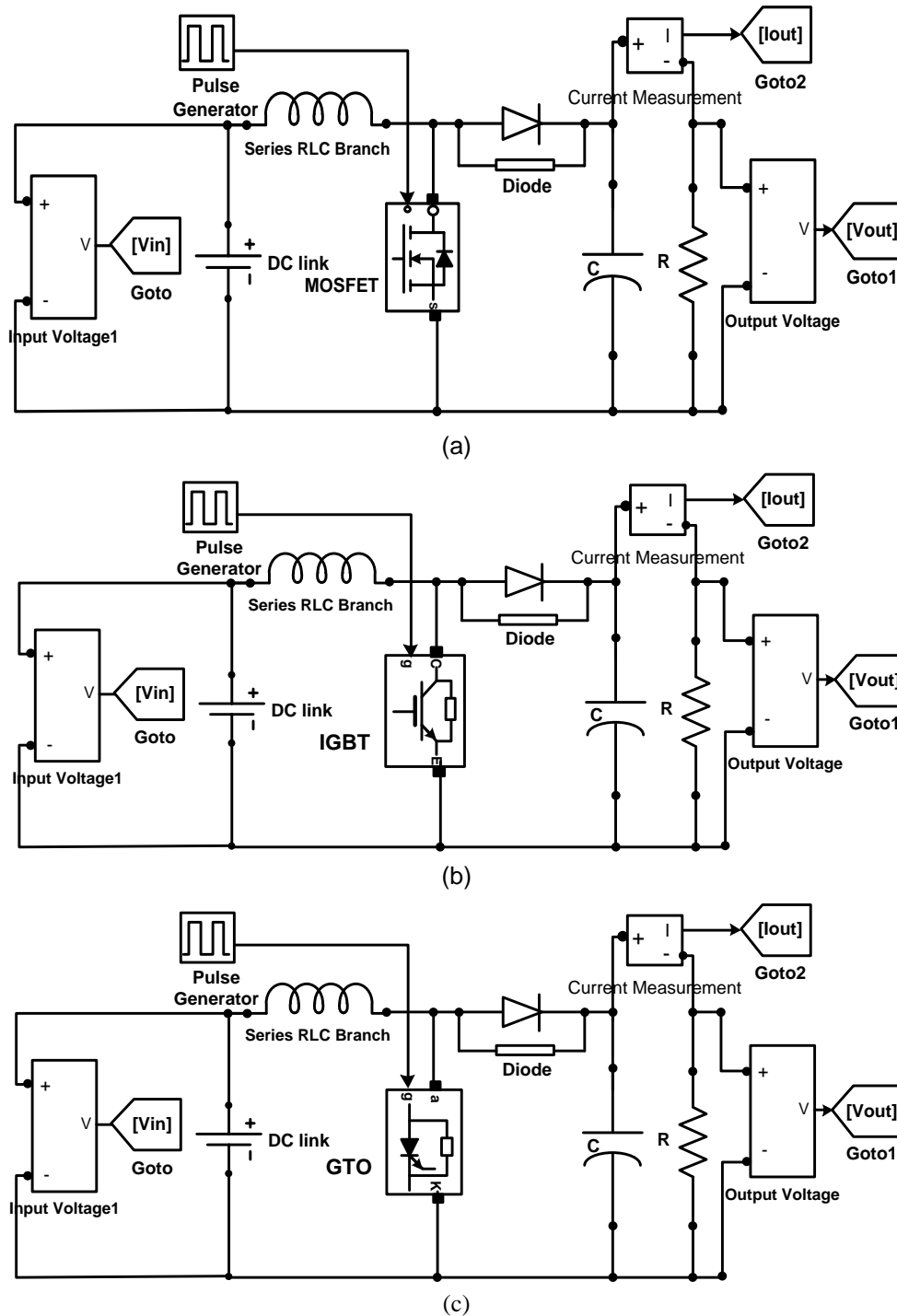


Figure 7. DC/DC Boost Converter Model; (a) MOSFET, (b) IGBT, (c) GTO

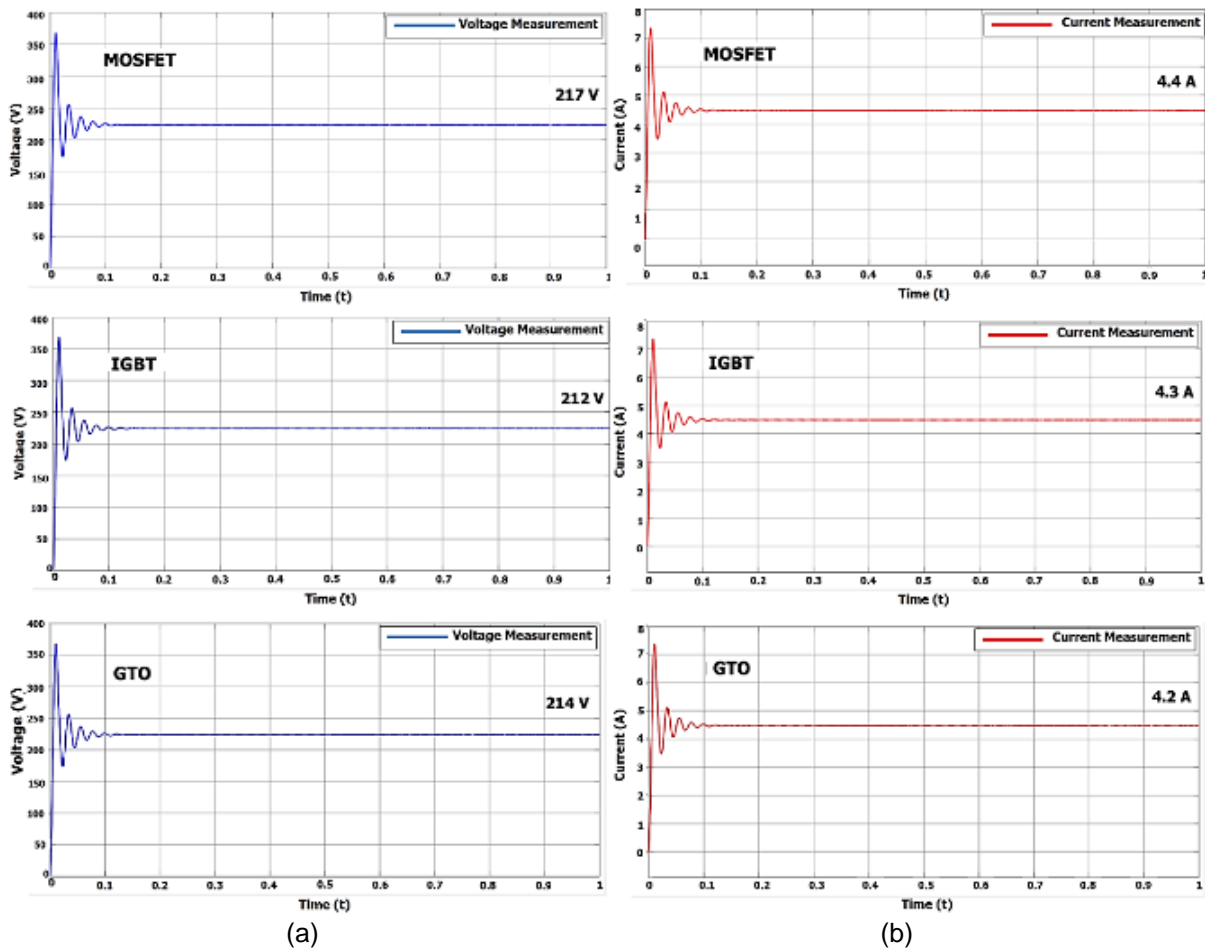


Figure 8. DC/DC Boost Converter Simulation Result; a) Voltage, b) Current

Figure 8 indicates DC-DC Boost Converter simulation using MOSFET results in predicted voltage and current with an improvement in voltage of 20,56%, with a voltage of 217 VDC and a current of 4.4 A relative to other devices. Generally, the current and voltage changes in each part are seen. Once the switch is opened, the current contained in the inductor will decrease due to impedance. So, the current that flows at the switch and at the load increases. The capacitor will also store energy in the form of a voltage at the same time. So, the output in the series should be much higher than the input.

Figure 9 shows a comparison of each circuit's output result (Voltage and Current) by using the parameter in Table 3. After the converter's process continues to the inverter block, DC output is converted to the AC. PWM type controllers use circuits to track the MPP of the PV module or the I-V array curve. The controller measures the charging conditions, adjusts the pulse, and generates the correct trigger signal for the switch present in the DC/DC converter circuit block.

Table 3. Switching Component Parameters

| No. | Components  | MOSFET    | IGBT        | GTO       |
|-----|-------------|-----------|-------------|-----------|
| 1   | Inductance  | 3 $\mu$ H | 266 $\mu$ H | 2 $\mu$ H |
| 2   | Capacitance | 2.5 mF    | 2 mF        | 2.7 mF    |
| 3   | Resistance  | 50 Ohm    | 50 Ohm      | 50 Ohm    |

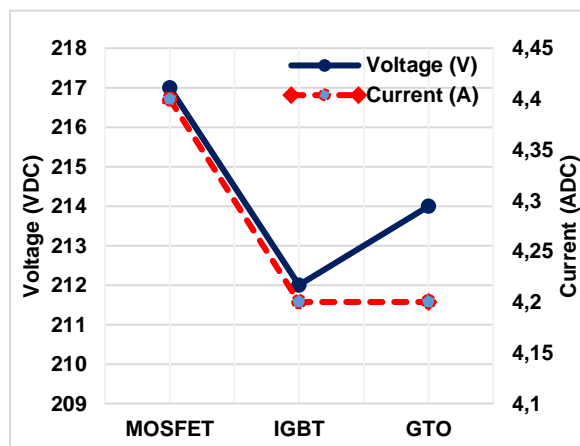


Figure 9. Testing Simulation Result

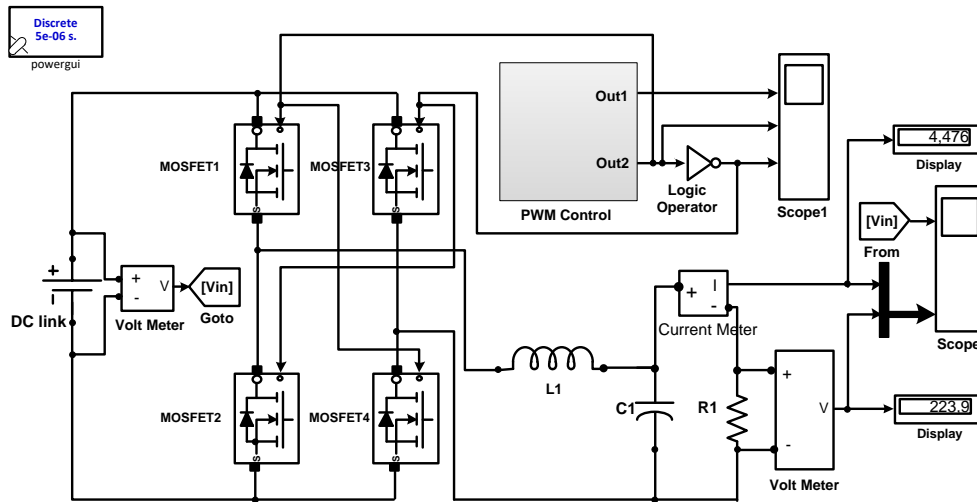


Figure 10. DC/AC Converter Model using MOSFET

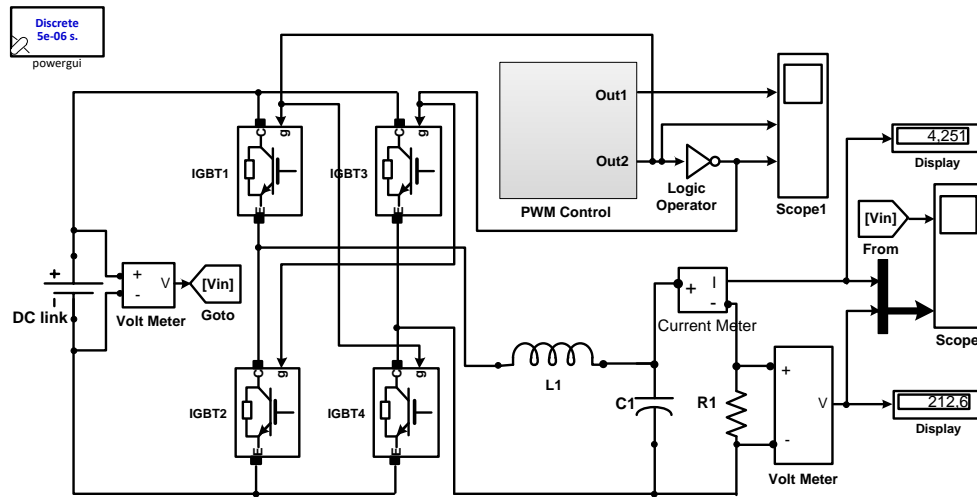


Figure 11. DC/AC Converter Model using IGBT

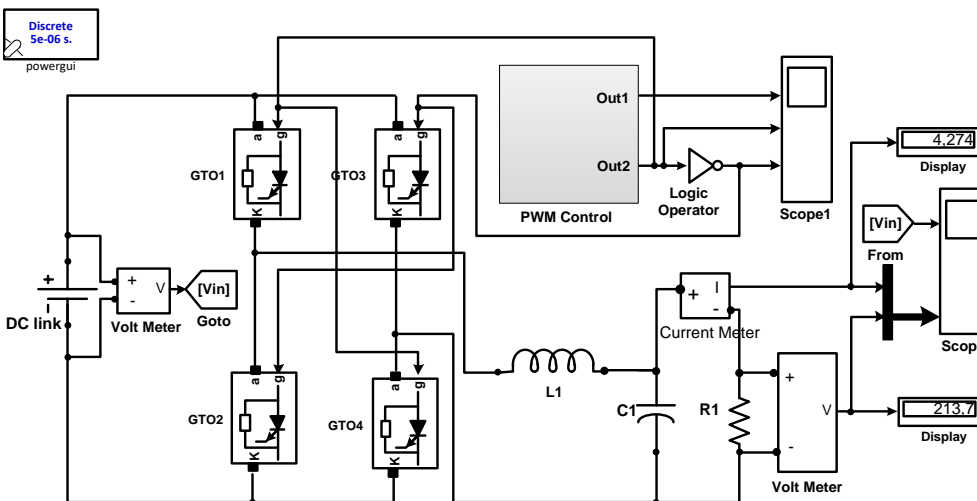


Figure 12. DC/AC Converter Model using GTO

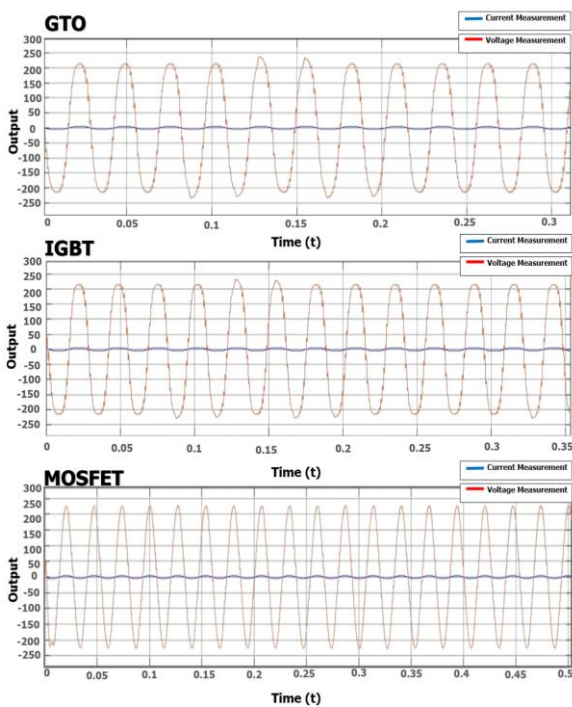


Figure 13. Inverter Simulation Output

### DC/AC Converter Simulation Result

DC/AC Converter circuit is modeled, using MOSFET, IGBT, and GTO switching. Figure 7, Figure 8 and Figure 9 is an inverter simulation circuit. The concept of the circuit is the line or direction of the current in the converter circuit branch. Some possibilities between the voltage and current source terminals will occur. A condition of relationship where current (I) flows from switch 1 to switch 4, then-current (I) flows from switch 2 to switch 3 and conditions where current and voltage are not connected. Conditions between switches 1, 2 and switches 3, 4 closings together may not occur. If this condition occurs, it will result in a short circuit. This controller is modeled and used to run electronic loads that require 110 or 230V AC. In this case, the PV system has the maximum power characteristics of a 100 W PV module arranged in 10 panels, so Pout's value is 100W multiplied by 10 panels producing 1000 Watt peaks. These results are divided by the results of the multiplication of the efficiency of the inverter. In general, inverters must be designed >93% (0.93), or we take the highest efficiency, which is  $\eta = 0.98$ . Each inverter charging is given a value for each component, as shown in Table 4, where each component's parameters are proposed to produce a near-perfect output. This circuit is simulated using several different values of impedance and capacitor parameters for each switching.

Table 4. Simulation Output of DC/AC Converter

| No. | Components | Voltage (VAC) | Current (A) | Freq. (Hz) |
|-----|------------|---------------|-------------|------------|
| 1   | MOSFET     | 227           | 4,4         | 50         |
| 2   | IGBT       | 212           | 4,2         | 52.6       |
| 3   | GTO        | 213,7         | 4,2         | 55.5       |

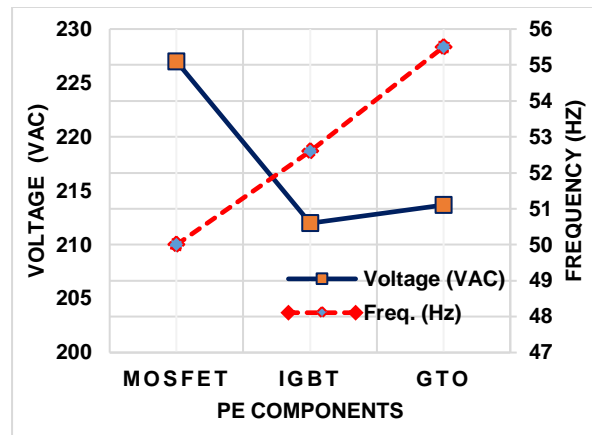


Figure 14. Output Voltage with Frequency of each Component

The converter's configuration is required to obtain the current source and voltage source's characteristics, voltage polarity, and current path following the input cycle. The current source or voltage source current is inverted under conditions S1 and S3 close and under conditions where S2 and S4 open or reverse conditions where S1 and S3 open and under conditions where S2 and S4 close. Selecting the switch S is determined from the current direction when S is closed (ON) and the voltage polarity at S is opened (OFF). Switching on the MOSFET, IGBT and GTO inverter circuit shown in Figure 10, Figure 11, Figure 12 produces several voltage waves and the output current approaches the Grid Connected criteria.

Figure 13 shows the inverter output results in the form of AC currents and voltages that are close to sinusoidal with currents and voltages of 4.4 amperes and 224 VAC, respectively. To get the current and voltage waves approaching the sine, the sinusoidal PWM control technique is used and each inverter is given a value for each component, and output shown by Figure 14. Tests using IGBT power electronic switching obtained output voltage and current with a value of 212 Volts AC and 4.2 Amperes. The circuit that uses GTO switching component values is almost the same as the MOSFET and IGBT circuits. The circuit simulation shows a sine wave with 50 Hz for MOSFETs, 52.6 Hz for IGBT, and 55.5 Hz for GTO.



## CONCLUSION

The conclusions drawn on a simulation for PV panels tested under STC are appropriate and comply with the system characteristics requirements, based on the results of simulations and testing carried out on the three types of power electronic components in a single-phase grid connected converter. Modeling of DC-DC Boost Converter has been carried out. According to the desired initial design, i.e., the inverter circuit's simulation tests that have been conducted agree with the same specifications as the 220V/50Hz PLN grid, and the inverter output frequency is the same as the 50 Hz grid frequency. A circuit model that meets the Grid-connected criteria by using MOSFET switching and can be implemented to Grid-connected with an efficiency of 96.7%.

## REFERENCES

- [1] C. P. Kandasamy, P. Prabu, and K. Niruba, "Solar Potential Assessment Using PVSYSY Software," in *International Conference on Green Computing, Communication and Conservation of Energy (ICGCE)*, India, 2013, pp. 667–672, DOI: 10.1109/ICGCE.2013.6823519
- [2] A. Purwadi, Y. Haroen, F. Y. Ali, N. Heryana, D. Nurafiat, and A. Assegaf, "Prototype Development of a Low Cost Data Logger for PV Based LED Street Lighting System," in *International Conference on Electrical Engineering and Informatics (ICEEI 2011)*, Bandung, Indonesia, July 2011, pp. 11–15, DOI: 10.1109/ICEEI.2011.6021693
- [3] H. R. Iskandar, E. Darmawan, Y. B. Zainal, G. Angga Setia, N. Winanti, and F. Haz, "Design of Solar Power Plant for Electrical Engineering Department Laboratory," *2019 2nd Int. Conf. High Volt. Eng. Power Syst.*, pp. 145–150, Oct. 2019, DOI: 10.1109/ICHVEPS47643.2019.9011041
- [4] A. F. Panchula, "Practical calculation of lost energy for large PV power plants," in *37th IEEE Photovoltaic Specialists Conference*, 2011, no. 3, pp. 002412–002414, DOI: 10.1109/PVSC.2011.6186435
- [5] A. Joshi, A. Khan, and A. Sp, "Comparison of half cut solar cells with standard solar cells," in *2019 Advances in Science and Engineering Technology International Conferences (ASET 2019)*, Dubai, United Arab Emirates, 2019, pp. 1–3, DOI: 10.1109/ICASET.2019.8714488
- [6] H. R. Iskandar, Y. B. Zainal, and S. Sambasri, "Study and Analysis of Shading Effects on Photovoltaic Application System," *1st Int. Conf. Ind. Electr. Electron. (ICIEE)*, vol. 218, no. 02004, pp. 1–8, 2018, DOI: 10.1051/mateconf/201821802004
- [7] H. Eteruddin, D. Setiawan, and Y. Z. Arief, "Effect of the Temperature on the Output Voltage of Mono-crystalline and Poly-crystalline Solar Panels," *SINERGI*, vol. 24, no. 1, pp. 73-80, 2020, DOI: 10.22441/sinergi.2020.1.010
- [8] S. Salman, X. Ai, and Z. Wu, "Design of a P-&O algorithm based MPPT charge controller for a stand-alone 200W PV system," *Protection and Control of Modern Power Systems*, vol. 3, no. 1, pp. 1-8, 2018, DOI: 10.1186/s41601-018-0099-8
- [9] M. H. Anowar and P. Roy, "A Modified Incremental Conductance Based Photovoltaic MPPT Charge Controller," in *2nd International Conference on Electrical, Computer and Communication Engineering, (ECCE)*, Bangladesh, 2019, no. 1, pp. 1–5, DOI: 10.1109/ECACE.2019.8679308
- [10] H. S. Moreira, J. L. De Silva, G. C. S. Prym, E. Y. Sako, M. V. G. Dos Reis, and M. G. Villalva, "Comparison of Swarm Optimization Methods for MPPT in Partially Shaded Photovoltaic Systems," in *2019 International Conference on Smart Energy Systems and Technologies (SEST)*, Porto, Portugal, September 2019, pp. 1-6, DOI: 10.1109/SEST.2019.8849145
- [11] H. D. Liu and C. H. Lin, "Maximum Power Point Tracking Method for PV Module under Wide Range Varying Irradiance Levels," in *2018 International Power Electronics Conference, IPEC-Niigata - ECCE Asia 2018*, Oct. 2018, pp. 1777–1781, DOI: 10.23919/IPEC.2018.8507975
- [12] A. Purwadi, A. Rizqian, R. Fachrizal, and N. Heryana, "Modeling of 1.6 kWp Single-Phase Grid-Connected Photovoltaic System," in *The 5th International Conference on Electrical Engineering and Informatics*, China, 2015, pp. 552–557, DOI: 10.1109/ICEEI.2015.7352561
- [13] Y. Yang and H. Wen, "Adaptive perturb and observe maximum power point tracking with current predictive and decoupled power control for grid-connected photovoltaic inverters," *J. Mod. Power Syst. Clean Energy*, vol. 7, no. 2, pp. 422–432, Mar. 2019, DOI: 10.1007/s40565-018-0437-x
- [14] H. R. Iskandar, S. Basuki, M. R. Hidayat, A. Daneraici Setiawan, D. Rukanda, and S. U. Prini, "Wireless Telemetry for Real-time Monitoring of Photovoltaic Application System using Monopole Antenna 3DRobotics Radio 915 MHz," *2019 IEEE 13th Int. Conf. Telecommun. Syst. Serv. Appl.*,

- Bali, Indonesia, Oct. 2019, pp. 277–281, Oct. 2019, DOI: 10.1109/TSSA48701.2019.8985518
- [15] H. R. Iskandar, S. Sambasri, D. I. Saputra, N. Heryana, A. Purwadi, and M. Marsudiono, "IoT Application for On-line Monitoring of 1 kWp Photovoltaic System Based on NodeMCU ESP8266 and Android Application," *2019 2nd Int. Conf. High Volt. Eng. Power Syst.*, Bali, Indonesia, Oct. 2019, pp. 230–234, Oct. 2019, DOI: 10.1109/ICHVEPS47643.2019.9011154
- [16] H. M. Al-Masri, A. Abu-Errib, W. R. Ayyad, and M. Ehsani, "On the PV module characteristics," in *International Symposium on Power Electronics, Electrical Drives, Automation and Motion (SPEEDAM 2016)*, Italy, June 2016, pp. 901–905, DOI: 10.1109/SPEEDAM.2016.7525948
- [17] H. R. Iskandar, A. Purwadi, A. Rizqiwani, and N. Heryana, "Prototype Development of a Low Cost Data Logger and Monitoring System for PV Application," in *The 3rd IEEE Conference on Power Engineering and Renewable Energy (ICPERE)*, Yogyakarta, 2016, pp. 171–177, DOI: 10.1109/ICPERE.2016.7904864
- [18] A. A. Zakri, N. Nurhalim, D. P. H. Simanulang, and I. Tribowo, "Photovoltaic Modeling Methods Based on Matlab Simulink Implementation," *SINERGI*, vol. 22, no. 1, pp. 1–6, 2018, DOI: 10.22441/sinergi.2018.1.001
- [19] A. Sangwongwanich, "A New Power Control Strategy for Grid-Friendly Single-Phase Photovoltaic Systems," *Master Thesis*, Aalborg University, 2014
- [20] L. Liang, W. Wang, Y. Jia, and S. Fu, "A cluster-based energy-efficient resource management scheme for ultra-dense networks," *IEEE Access*, vol. 4, pp. 6823–6832, 2016, DOI: 10.1109/ACCESS.2016.2614517
- [21] M. Ali, A. Yousaf, and F. Usman, "Design and Simulation of Power Electronic Controller for Grid Connected PV Array with maximum power point tracking (MPPT)," in *the 8th International Renewable Energy Congress, (IREC 2017)*, Dead Sea, Jordan, 2017, no. Irec, pp. 6–9, DOI: 10.1109/IREC.2017.7926043
- [22] P. K. Vineeth Kumar and K. Manjunath, "Analysis, design and implementation for control of non-inverted zeta converter using incremental conductance MPPT algorithm for SPV applications," in *Proceedings of the International Conference on Inventive Systems and Control (ICISC 2017)*, India, 2017, pp. 4–8, DOI: 10.1109/ICISC.2017.8068662
- [23] J. A. Ramos-Hernanz, J. M. Lopez-Guede, E. Zulueta-Guerrero, N. Bizon, F. Oterino-Echavarri, and A. Larrea, "Study of the behavior of the Incremental Conductance algorithm for MPPT," in *Proceedings of the 8th International Conference on Electronics, Computers and Artificial Intelligence (ECAI 2016)*, Romania, July 2016, pp. 1–6, DOI: 10.1109/ECAI.2016.7861152
- [24] S. Palanidoss and T. V. S. Vishnu, "Experimental analysis of conventional buck and boost converter with integrated dual output converter," in *International Conference on Electrical, Electronics, Communication Computer Technologies and Optimization Techniques (ICEECCOT)*, New Delhi, India, Dec. 2017, pp. 323–329, DOI: 10.1109/ICEECCOT.2017.8284521
- [25] H. R. Iskandar, A. Prasetya, Y. B. Zainal, M. R. Hidayat, E. Taryana, and G. Megiyanto, "Comparison Model of Buck-boost and Zeta Converter Circuit using MPPT Control Incremental Conductance Algorithm," in *2020 International Conference on Sustainable Energy Engineering and Application*, Jakarta, Indonesia, Nov. 2020, pp. 185–190, DOI: 10.1109/ICSEEA50711.2020.9306121